HHS Public Access

Author manuscript

Dev Neurosci. Author manuscript; available in PMC 2017 October 28.

Published in final edited form as:

Dev Neurosci. 2016 ; 38(4): 295–310. doi:10.1159/000449035.

Development of electrophysiological properties of nucleus gigantocellularis (NGC) neurons correlated with increased CNS arousal

Xu Liu[1,2], **Donald W. Pfaff**[1], **Diany P. Calderon**[1], **Inna Tabansky**[1], **Xin Wang**[2], **Yun Wang**[3], and **Lee-Ming Kow**[1]

[1]Laboratory of Neurobiology and Behavior, The Rockefeller University, New York, NY 10065

[2]Neurology Department, Zhongshan Hospital, Fudan University, Shanghai, China

[3]Institute of Brain Science and State Key Laboratory of Medical Neurology, Fudan University, Shanghai, China

Abstract

Many types of data have suggested that neurons in Nucleus Gigantocellularis (NGC) in the medullary reticular formation are critically important for CNS arousal and behavioral responsiveness. To extend this topic to a developmental framework, whole-cell patch-recorded characteristics of NGC neurons in brainstem slices, and measures of arousal-dependent locomotion of postnatal day 3 (P3) to P6 mouse pups were measured and compared. These neuronal characteristics developed in an orderly, statistically significant monotonic manner over the course of postnatal days 3–6 (P3-P6): (i) proportion of neurons capable of firing action potential (AP) train; (ii) AP amplitude; (iii) AP threshold; (iv) amplitude of inward and outward currents; (v) amplitude of negative peak currents; and (vi) steady state currents (in I-V plot). These measurements reflect the maturation of sodium and certain potassium channels. Similarly, all measures of locomotion, latency to first movement, total locomotion duration, net locomotion distance and total quiescence time also developed monotonically over P3-P6. Most important: electrophysiological and behavioral measures were significantly correlated.

Interestingly, the behavioral measures were not correlated with frequency of excitatory postsynaptic currents or the proportion of neurons showing these currents, responses to a battery of neurotransmitter agents, or rapid activating potassium currents (including I_A).

Considering the results here in the context of a large literature on NGC, we hypothesize that the developmental increase in NGC neuronal excitability participates in causing the increased behavioral responsivity during the postnatal period from P3 to P6.

Keywords

Arousal; developing brain; behavior; brainstem reticular formation; electrophysiology; ion channel; neonatal; neurotransmitter; nucleus gigantocellularis (NGC); patch clamp

Corresponding author: Lee-Ming Kow, Ph.D., The Rockefeller University, 1230 York Avenue, Box 336, New York, NY 10065. kowl@rockefeller.edu, Phone: 212-327-8669, FAX: 212-327-8664.

Introduction

Some classical, fundamental problems in neuroscience address questions about the mechanisms necessary for a wide variety of behaviors to be initiated. A long history of behavioral research has focused on the capacities of mouse and rat neonatal pups. This line of work has matured into the presentation of specific questions, for example, about the effects of endocrine disruptors [1], neonatal androgen levels [2], and roles for neonatal ultrasonic vocalizations [3]. Our study is novel in that it is the first to focus on behavioral arousal for its own sake and for its correlation with patch clamp, whole cell recordings of neuronal electrical activity.

Adequate CNS arousal, sometimes conceived as “generalized arousal” [4], has been importantly addressed by many neuroscientists and molecular biologists [5–8]. One particularly critical time at which adequate CNS arousal is required must be at the onset of behavioral responsiveness soon after birth. During the course of animal preparations for patch clamp recording experiments, we noticed a steady transition in behavioral responsiveness during the period from postnatal day 3 (P3) to P6, and decided to study this developmental time period systematically.

What neuronal changes might accompany, or even cause this early transition in the activation of movement? One prominent possibility would be the large medullary reticular neurons in Nucleus Gigantocellularis (NGC). It has been argued [9] that these neurons play a central and fundamental role in generalized arousal. They possess the neuroanatomical connectivity, physiological responsivity and arousal-related gene expression to do the job of facilitating the initiation of a wide variety of behaviors.

Connectivity

NGC neurons contribute importantly to ascending arousal pathways in the brainstem, both those that will travel the medial forebrain bundle to the basal forebrain and to those which will activate the central thalamus [10]. Likewise, axons descending from NGC travel to all levels of the spinal cord, with terminations bilateral [11–13]. Some NGC neurons show bifurcating axons, thus having the capacity to contribute to both ascending and descending arousal pathways [14].

Responsivity

Electrical recordings of single NGC neurons in awake behaving animals showed that these neurons could respond to all sensory modalities tested [15]. Moreover in animals standing quietly, neurons were observed to start firing just before movement [16]. Optogenetic activation of a portion of NGC neurons causes activation of the cortical EEG and the onset of movements even in anesthetized animals [17]. Importantly, deletion of NGC neurons that express the Chx10 gene hampered movements in mice [18].

Gene expression

Genes coding for arousal-related receptors, those serving increased arousal (e.g. Orexin receptor-1) or decreased arousal (e.g. opioid receptors) are expressed in NGC neurons [12].

The firing rate/patterns of brainstem NGC neurons have been shown to be correlated various movement-REM (rapid eye movement) electroencephalogram (EEG) [16,19]. Conversely, either direct electrical stimulation [20], pharmacologic or optogenetic disinhibition of NGC neurons [17] caused an elevation of CNS arousal as measured by the cortical EEG.

Thus, we hypothesized that changes in NGC electrical excitability would be related to the onset of movements during the important developmental period of P3-P6. Following measurements of the initiation of movement during this period we recorded several measurements of electrical excitability of NGC neurons in the same animals.

Materials and Methods

All procedures in handling and treating the animals were approved by The Rockefeller University's Animal Care and Use Committee in accordance with the Animal Welfare Act and the Department of Health and Human Services' "Guide for the Care and Use of Laboratory Animals".

Animal

Three- to six-day postnatal (P3 – P6) C57BL/6J mouse pups were used. The age range was chosen based on: 1) to cover the period of important progress of arousal-related behaviors and of neuronal characteristics, which plateaued or nearly so at P6; and 2) also to guarantee successful patch clamp recordings from nucleus gigantocellularis (NGC) neurons, which are easy to visualize before the growth of reticular fibers in adults. All animals were maintained in air-conditioned rooms with temperature controlled at 23 ± 2°C, under a reversed light/dark cycle with lights on from 5:00 pm through 5:00 am. Animals were housed in plastic cages, and given water and food *ad libitum*. All experiments including whole-cell patch clamp recording and behavior measurements were performed between 9 am and 4 pm (during the light period of the daily light cycle).

Brain slice preparation

Brainstem slices containing NGC from young mouse pups were prepared as described previously [15,21,22]. Briefly, mice were deeply anesthetized with isoflurane (used with an Anesthesia Machine from LEI medical Co.) and decapitated to quickly remove the brain The brain was then rinsed and chilled with ice-cold (4°) aerated (95% 02/5% CO2) sucrose artificial cerebrospinal fluid (ACSF) for about one minute. Sucrose ACSF is the solution that has all the NaCl in the ACSF replaced by sucrose in order to prevent damage of neurons from over excitation. After removing the pia mater from the ventral surface, the brainstem was blocked out and fixed on the cutting stage of a Vibratome (model 1000 Plus, The Vibratome Company, St Louis, MO) using Krazy Glue. The brainstem immersed in ice-cold sucrose ACSF and 250-μm-thick brainstem slices containing NGC were collected from anterior one-third of medullary reticular formation, matching the placement of the electrodes implanted for *in vivo* chronic recording [17]. Slices were then stored in ACSF at room temperature for at least 1 hour before recording. The constituent of ACSF is (in mM): NaCl, 126; KCl, 5; NaH_2PO_4, 1.25; $CaCl_2$, 2; $MgCl_2$, 2; $NaHCO_3$, 26; dextrose, 10; and oxygenated with 95% O_2/5% CO_2.

Whole-cell patch clamp recordings

The brain tissue slice was transferred to and placed on the bottom of the recording chamber fixed to the stage of an upright microscope (Olympus BX50WI). The slice was superfused with oxygenated ACSF at about 2ml/min. All recordings were performed at room temperature. Neurons in the slice were visualized with infrared differential interference contrast (IR-DIC) optics. The NGC was located under low magnification (40x) and guided by landmarks. NGC neurons were selected and patched under higher magnification (400x) with electrodes pulled from Borosilicate glass pipettes (G8515OT-4, Warner Instruments, Hamden, CT) using a Narishige PP-830 puller. Electrode resistance was 5–7 MΩ when filled with an internal solution composed of (in mM): K-Gluconate, 140; EGTA, 5; $MgCl_2$, 2; $NaHCO_3$, 0.6; HEPES, 10; Mg-ATP, 2; Na_2-ATP, 2; $CaCl_2$,1; Na-GTP, 0.3; and sucrose, 8.3. The liquid junction potential between pipette and bath was not measured, but was calculated using Clampex's Junction Potential calculation tool. However, since our most interesting results turned out to be current amplitudes that are not affected by that correction, no correction, on-line or off, was performed. Whole-cell current or membrane potential (Vm) was amplified with Multiclamp 700B and recorded and analyzed with Clampex and Clampfit, respectively (Axon Instruments).

Experimental procedures

Once a whole-cell configuration was established, the resting membrane potential (Vm) was measured and then subjected to membrane test. If the patch met the following criteria: Access resistance (Ra) ≤15 MΩ, leak current ≤50 pA, and resting Vm to be equal or more negative than −45 mV, then the recording proceeded to undergo tests with the following series of protocols. First, a 10-sweep current step protocol to induce action potential (AP). The current was held at zero and first level at −20 pA followed by nine 10-pA increment steps. Second, a single voltage step from −70 mV to 0 mV for 10 ms to induce inward and outward currents. Third, a 14-sweep voltage step protocol with holding potentials (Vh) at −70 mV was used for constructing I-V curves. The first level (sweep) was −110 mV in order to activate K^+ currents activated by hyperpolarization. This was followed thirteen 15-mV increments. Fourth, a voltage step protocol the same as the third protocol, except that the Vh is −40 mV, at this voltage the rapid activating K^+ currents are inactivated [23]. The last two protocols are illustrated in the Results section. Fifth, a gap-free protocol with Vh at −70 mV was employed to record excitatory postsynaptic current (EPSC). Sixth and finally, a gap-free protocol with current clamped at around −70 mV to study responses of NGC neurons to a battery of bath-applied neurotransmitter receptor agonists (to be referred to as 'test agents' for brevity).

Test agents

Neurotransmitter agonists, including N-methyl-D-aspartate (NMDA), glutamate (Glut), Phenylephrine (PhE), histamine (HA), γ-aminobutyric acid (GABA) were used. They were dissolved with ACSF, first as stock solutions then diluted before use to final concentrations of: NMDA 20 μM, Glut 50 μM, PhE 100 μM, HA 100 μM, and GABA 30 μM. They were applied through the bath. All test agents and the materials for internal and bath (ACSF) solutions were purchased from Sigma Chemical Company.

Measurements of neuronal characteristics

From the current step protocol, the threshold and the amplitude of the AP with the shortest latency were measured. The threshold is defined as the intersection of the extension of the depolarization slope and the slope of the rising phase of the AP. From the threshold to the peak of the AP is its amplitude. The amplitude of inward and outward currents induced by single voltage step are measured from the base line. Results from multiple voltage steps were plotted into I-V curves with the standard Clampfit program. The troughs and peaks, respectively, of the inward (negative) and outward (positive) currents are referred to as Negative and Positive peak currents, respectively. The average of the last 100 ms of each trace is plotted as Steady State current. Amplitudes of the rapid and fast activating K^+ currents, which are defined in the Results section, are measured accordingly. Currents measured were not scaled to cell size. The EPSC trace was analyzed with a Minianalysis program (Synaptosoft Inc.) to obtain the frequency, amplitude and area of EPSCs recorded.

Behavioral assay

A separate group of 14 × 4 (n=14 for each age) of P3- to P6-day old male and female young μouse pups were used. They were allowed to acclimatize to the observation room for at least half an hour before testing. Tests were performed under dim (red) light. All observations were done during the dark phase between 9 am and 4 pm. For the behavioral assay, a pup was placed in the center of a hyaline cube box with a 16 cm x 16cm x 12 cm dimension and after the latency to the initial movement was recorded (= time 0) it was further observed for 900 seconds for movement and quiescence durations. Entire observation was recorded and saved on a computer for review. The latency to first movement was recorded, and then the duration of total movement and quiescence duration were measured. The movement duration is the sum of the time when: a) pup raised its head, b) shifted its limbs, c) circled or d) crept forward. The “quiescence” time was recorded as the total time the animal lay absolutely still, without any movement. The net distance between starting and final locations was measured at the end of the observation.

Data Analysis

Data are presented as mean ± SEM (n). One-way ANOVA or chi-square test was used to compare two samples. Whether changes from P3 to P6 in any measurement were significant was tested with Mann-Kendall test for Trend (MKT). Correlations between any electrophysiological measure and any behavioral measure were tested with Spearman Rank Correlation Coefficient test. The significance level was set at $P < 0.05$ two-tailed, unless otherwise stated.

Results

Current injection-induced Action Potentials (APs): their amplitude and peak level increased (and threshold decreased) over days P3-P6

The application of current steps is intended to study the development of the neuron’s capability to fire APs, and by inference, the development of Na^+ and Ca^{++} currents. Injection of currents could, depending on neurons and their age, induce no AP, a single AP

and or a train of APs (Fig. 1 insert). As illustrated in Fig. 1, NGC neurons' ability to induce AP trains increased monotonically from P3 to P6. Indeed, the percentage of neurons capable of firing AP trains increased significantly from 17% (2 in 12) on P3, 33% (6 in 18) on P4, 38% (6 in 16) on P5, to 80% (12 in 15) on P6 (Table 1). The proportion of neurons capable of firing a single AP was highest on P3, but the decline thereafter was not orderly (Fig. 1 and Table 2). Correspondingly, there was a non-significant trend for the proportion of silent NGC neurons (incapable of firing an AP) to decrease from P3 toward P6 (Fig. 1).

Of other characteristics of induced APs from NGC neurons defined in the Methods, the amplitude increased and the threshold of first AP decreased, steadily and significantly ($p=0.042$) from P3 through P6 (Table 1, Action potential).

Inward and outward currents increase from P3 to P6

As in the case of AP characteristics, both inward and outward currents of NGC neurons, induced by the one-step depolarization, increased steadily and significantly ($p=0.042$) from P3 through P6 (Table 1, Currents by single voltage step).

The amplitude of both types of currents mentioned above on P6 are significantly greater than those on P3 (ANOVA, all p's <0.05, Table 1).

Changes in currents generated by I-V steps

A typical example of currents generated by the I-V steps at the holding potential (Vh) of −70 mV is illustrated in Fig. 2A, and the resulting I-V plot with positive and negative peak and steady state currents are presented in Fig. 2C. As shown in Fig. 2C, the negative trough maximal current (NPk) was elicited at several commanding voltage steps but was greatest at −35 mV, indicating that, in this case at least, the NPk was mainly Na^+ currents and most likely also some Ca^{++} currents. In slice recording, where imperfect space clamp sometimes occurs, the inward currents may also contain "axial currents" (indicated by the out-of-place inward current in Fig. 2Aa) induced by an axonal action potential escaping the imperfect space clamp [24]. The axial current may contain other currents than the main Na^+ current. Having flowed through small neurites into the large soma, axial current would be dispersed and therefore would not affect our main finding (see below).

Like the inward currents induce by single voltage step (from −70 mV to 0 mV for 10 ms), both NPk currents obtained with Vh at −70 and −40 mV also increased (became more negative) monotonically and significantly ($p=0.04$) from P3 through P6 (Table 1). The single voltage step is too brief to allow for axial current to contaminate the inward current the voltage step evoked. When neurons are held at −40 mV, near the AP threshold, the axonal AP and, hence, the axial current are inactivated [24]. Therefore, the inward currents measured with holding potential (Vh) at −40 mV are devoid of the "axial current" (note that the "axial current" is no longer detectable in Fig. 2Bb). The facts that the NPk obtained with Vh at −70 mV is similar to these two currents indicated that the contamination, if any, by the axial current did not affect the main finding of a monotonic increase. Similar to inward currents, the steady state (SSt) currents also increase in the same fashion (Table 1). The monotonic changes of these two types of currents are correlated with the similarly monotonic changes of arousal-related behaviors (Table 3). In contrast, the positive peak

currents, which are a combination of steady state and other currents (see below), did not change in a monotonic fashion, although their amplitude are significantly ($p < 0.01$) larger on P6 than on P3 (Table 2).

The rapid activating current was determined and measured as following. In the typical example showing in Fig. 2A, one can see some traces (from traces 6 through 11, see Fig. 2 inset Aa), have a sharp upswing upon the application of voltage steps with holding potential (Vh) at −70 mV (see Fig. 2 insert Cc). These rapid outward currents were abolished when the holding potential was set at −40 mV (Fig. 2 insert Dd), which would inactivate rapid activating and rapid inactivating K^+ currents [23]. This is clearly shown in Fig. 2B and the inset Bb, where traces rise smoothly to a gentle top without any trace of a sharp upswing. These results are also reflected in the corresponding I-V plots. In Fig. 2C, the plot for traces in Fig. 2A, starting from commanding voltage −35 mV on there are gaps between positive peak (PPk) and steady (SSt) currents. In contrast, in Fig. 2D generated with Vh at −40 mV, these gaps disappear from commanding voltages −35 mV through 25 mV, indicating that the gaps represent the amplitude of the rapid current. The gap increases and then decreases with the maximum at, in this example, −5 mV, highlighted in red in Fig. 2A and insert a. This largest gap is regarded as the amplitude of the rapid activating and inactivating currents, commonly known as A-current.

The amplitude of the rapid activating and inactivating currents varied over the age of P3 through P6, but not monotonically (Table 2) and the changes are hence not correlated with the changes of arousal-related behaviors that are all developing monotonically (Table 3).

Fig. 2 also illustrates the existence of another outward current. In Fig. 2A, numbers 3, 4 and 5 traces from the top, a secondary increase in current after the rapid peak is visible. These increases persist much longer (slow inactivating) than the rapid activating currents and are reflected by the nearly parallel PPk and SSt current in the I-V plot from 40 mV through 85 mV (Fig. 2C). These currents are not inactivated by raising the Vh to −40 mV (Fig. 2B) and that contributes to the later (beyond 25mV) separation of PPk and SSt curves in the I-V plot (Fig. 2D), hence they are distinct from the rapid activating currents. Based on these characteristics, these currents are referred to as the fast activating and slow inactivating current and are measured as the difference between the maximal (at 85 mV) PPk and SSt currents generated by protocol with Vh at −70 mV (Fig. 2C). Like rapid activating currents, the variation of fast activating currents over P3 through P6 is not in the form of a monotonic change (Table 2), and thus the change was not correlated with the monotonic changes of arousal-related behaviors.

Absence of significant changes of EPSCs recorded over P3-P6

EPSCs of NGC neurons were recorded to assess their connections with other neurons. Typical examples for the absence and the presence of EPSC are presented in Fig. 3A and 3B, respectively. Contrary to our expectation, the amplitude and the area of EPSCs examined decreased monotonically and significant statistically over the observation period from P3 through P6 (Table 1). However, the percentages of neurons showing EPSCs were steady over the observation days (Table 2), indicating that the neuronal connections are stabilized. This

indication is supported by the lack of significant change over days in the EPSC frequency (Table 2) that reflects the stable pre-synaptic conditions.

The responsiveness of NGC neurons to a battery of neurotransmitter agents virtually did not change over P3-P6

As illustrated in Fig. 4, all the test agents used, including GABA, evoked depolarization, even if the NGC neuron was incapable of firing action potential. Of all the neurons tested, regardless of age, NMDA (20 μM) is the most effective, stimulating all 29 neurons tested (100%) (Fig. 4A). This is followed by 96% (or 26 of the 27 neurons tested) by PhE (100 μM), then 90% (or 26/29) by HA (100 μM), 57% (or 17/25) by Glut (50 μM) and lastly 57% (16 in 28) by GABA (30 μM) (Fig. 4, B–E, respectively). Similar application of vehicle (ACSF) never had an effect (Fig. 4F). It is surprising to find that Glut, even at higher concentrations, was less effective than NMDA in depolarizing NGC neurons.

Findings that both NMDA and Glut evoked depolarization are to be expected as they both are excitatory agents. So are those of PhE, which is an agonist for adrenergic receptor α_1-subtype that mediates depolarization/excitation [25,26]. The seemingly unusual finding of GABA inducing depolarization is actually not surprising [27–29] since, in rat hippocampus, GABA induces excitation from P1 through at least P7 before inducing hyperpolarization when the animal becomes more mature (see [29] and the references therein). The mechanism of GABA excitation is twofold. First (i.) it induces a net outward flux of Cl^-, resulting in a membrane depolarization, (ii.) that subsequently opens voltage-gated Ca^{2+} channels for further depolarization (see [29] and the references therein). In the brain, HA has at least three receptor subtypes, H1 mediating depolarization and H2 and H3 inducing hyperpolarization [30]. The fact that HA was found to induce only depolarization indicates that H1, but not H2 or H3, is already developed in these young pups.

Relevant to the main line of thought in this study is the lack of change in other neurotransmitter actions over the days of experimentation (Table 2). NMDA stimulated all neurons: on P3 (n=8), P4 (n=8), P5 (n=6) and P6 (n=7). PhE stimulated all 6 neurons on P3, all 8 on P4, all 6 on P5 and 6 out of 7 neurons on P6. HA stimulated 5/5 on P3, 8/9 on P4, 5/6 on P5 and 6/7 on P6. Responsiveness to Glut are 4/6, 5/7, 4/6 and 4/6 from P3 through P6, respectively. GABA stimulated 2/7, 6/8, 4/6 and 4/7 on P3 through P6, respectively.

Firing capability of hippocampal CA1 neurons

To determine whether the development of AP characteristics also occurs from P3 to P6 in other neuronal types, to supplement the existing literature (see Discussion), CA1 neurons from hippocampus were also studied. Eight CA1 neurons from P4 mice were recorded and all 8 were capable of firing APs (Fig. 5); 5 (63%) fired AP trains and 3 (37%) fired a single AP. This is in contrast with NGC neurons, which at P4, only 33% were able to fire any AP. These comparisons suggest that, as expected, not all neurons in the brain developed in synchrony with NGC neurons or with the behavioral changes (see Discussion).

The capacity for behavioral arousal of mouse pups increases during days P3-P6

All four measures of the initiation and maintenance of mouse movements changed monotonically and in significant manner (all p's = 0.04) over the observation days P3 through P6 (Table 3). Total quiescence duration decreased and total movement duration increased steadily, from P3 to P6 (Fig. 6). Similarly, the latency to the first movement after start of the assay was decreased, and the net movement distance increased steadily from P3 through P6; and the results of P6 vs. P3 are significantly different (Fig. 7A).

Comparisons between NGC recordings and behavioral measures

To determine whether there is any correlation between NGC neuronal characteristics recorded and the animal behaviors measured, the statistically conservative Spearman rank correlation coefficient test was employed. We first compared the neuronal characteristics that had P3-P6 significant ($p<0.05$) developmental changes, including capability to fire AP trains, AP amplitude, threshold to AP, amplitude of inward and out ward currents, amplitude of negative peak current (see Table 1); now compared to all measures of behaviors, including latency to first movement, quiescence duration, movement duration and distance, all of these having significant (P3-P6 changes) (see Table 3). These comparisons show that each and every one of these neuronal characteristics is significantly correlated with each and every one of the behavioral measures (Table 3). Fig. 7B illustrates an example of such correlation between NGC neuronal capability to fire AP trains and movement duration. Correlations between the AP train capability with movement distance and the reversal of the latency to first movement are also obvious by comparing traces in Fig. 7B to those in 7A.

In contrast, none of the neuronal characteristics *without* a significant monotonic developmental P3-P6 change was correlated with any of the behavioral measures. Such NGC neuronal characteristics include amplitude of positive peak, rapid and fast activating currents, negative peak position, all characteristics of EPSCs, and responses to any neurotransmitter agents tested (Table 2).

DISCUSSION

In the present study, we found several interesting results. First, among the electrophysiological characteristics of NGC neurons studied, some changed monotonically during the time interval day P3 through P6 (Table 1); while others did not (Table 2). Second, *all* the arousal-related behaviors observed showed a statistically significant monotonic change during P3 through P6 (Table 3). Third, each and every one of the behavioral measures correlated with each and every one the neuronal characteristics that changed monotonically during P3-P6 (Table 3). These correlations allow us to argue, in the context of a robust literature (see below), that NGC neurons play a critical, causal role in the initial development of arousal-related behavior in the neonate.

Major findings

Electrophysiology—The present study is the first report on the electrophysiological characteristics of NGC neurons in the neonatal stages, although studies on young adults had been reported [31,32]. Electrophysiological characteristics of NGC neurons that changed in

monotonic fashion during P3-P6 include the increases in the capacity of to fire AP trains (Fig. 1), the amplitudes of APs, the inward currents induced with a single voltage step (Table 1) and both sets of negative peaks (inward currents) from the I-V plots measured at Vhs of −70 and −40 mV (Table 1) to address a question about axial current from incompletely clamped neurites. All of these changes during neuronal development have been reported for other types of neurons, namely the development of mouse Purkinje cells *in vivo* [33] and *in vitro* [34], rat Purkinje cells *in vitro* [35], rat cortical pyramidal neurons [36], forebrain neurons derived from human induced pluripotent stem cells [37], neurons differentiated *in vitro* from embryo stem cells [38] and embryonic stem cells [39], spinal motor neurons from human embryonic stem cells [40] and a cell line, NG108-15 cells [41]. Nearly all of these reports attributed some or all of these changes in neuronal characteristics to the increase in the expression of Na^+ channels [34–37,39–41]. The kinetics of these channels did not seem to matter [36]. Also, we [42] and others [43,44] have found that the inward currents induced with the same protocol used in the present study are virtually all composed of Na^+ currents. The fact that the changes of these characteristics correlated with the development of arousal-related behaviors during P3-P6 therefore indicates that the development of NGC neurons' Na^+ channels plays an important role in the progress of arousal during this critical arousal development "time window".

We found that all of our behavioral measures (Table 3) correlate with neuronal capability to fire AP trains (Table 1), but not with the simple occurrence of single APs (Table 2). This means that the increase in the expression of the Na^+ channel we observed, while essential for the maturation of APs, is not sufficient for enabling NGC neurons to fire AP repetitively in trains. This has also been reported for pyramidal neurons derived from stem cells, in which Na^+ currents are not correlated with whether neurons fire single, multiple or long trains of APs [39]. It is to be noted that certain subtypes of Na^+ currents, such as the persistent (I_{NaP}) [45,46] and the resurgent Na^+ currents [47,48], have been reported to enable or facilitate at least certain types of neurons to fire AP repetitively into trains. These currents were not singled out for observation in the present study, and hence whether they were present in the Na^+ currents we observed is not known. In hippocampal pyramidal neurons, repetitive firing that resulted in an AP train was shown to be regulated by rapid activating K^+ channels [49,50]. In the present study, rapid activating K^+ currents were observed throughout P3-P6, but to our surprise they varied irregularly (Table 2) and were not correlated with neuron's capability to fire AP trains or with the development of arousal-related behaviors. This lack of correlation also applies to the fast activating K^+ currents, which also varied irregularly (Table 2). The different results may be due to differences in the kinds of neurons (mouse NGC vs rat hippocampal pyramidal), and/or differences in ages (P3-P6 for mice vs P5-P12 for rats). The major remaining K^+ current that regulates repolarization and hence, the frequency of AP, is the delayed rectifier current. This current constitutes most, if not the entirety of the steady state current in the I-V chart and the positive currents elicited by the single voltage step. In the present study, this K^+ current - - the delayed rectifier current - - was found to increase monotonically (Table 1) and correlate with neuronal capacity to fire AP trains (Table 3), which are generally regarded as a unique functional feature of mature neurons [39,51–53]. Thus, the monotonic increase in the expression of Na^+ in combination with the development of delayed rectifier K^+ channels in NGC neurons are the major

contributors for the process of firing AP trains. Below we discuss its causative role in the development of arousal-related behaviors.

The significant correlations between the development of electrophysiological characteristics of NGC neurons and several behavioral measures of arousal imply that NGC neurons are involved in the development of behavioral arousal in the neonate. Three other cell types do not follow this time course: **(i.)** Purkinje cells were already capable of firing AP trains on P3-P4 [35,54] and are not inducers of movements [55]. Purkinje cells [34] and cerebral cortical pyramidal neurons [36], both involved in motor regulation like NGC neurons, appear to develop well ahead of NGC neurons. **(ii.)** Similarly, rat cortical pyramidal neurons could be induced to fire TTX-blockable AP trains as early as P1 [36]. **(iii.)**To check another type of neuron with large cell bodies (like our NGC cells), we recorded from hippocampal CA1 in slices prepared from P4 mouse pups (see Results). At P4, NGC neurons were *least* likely to fire AP (Fig. 1). In contrast, all 8 CA1 neurons fired APs at P4, 38% (3/8) fired single AP and 62% fired AP trains. CA1 neurons recorded from rat brain slices were already firing AP trains at P2 [56]. From these comparisons it appears that the development of NGC neuronal characteristics over P3-P6, correlated convincingly with the development of behavioral arousal, has some degree of specificity.

Behavior—We examined the quiescence, wake and movement times of neonatal mice from P3 to P6. We found that, during this period, the total duration of movement and the net distance of movement increased monotonically - the quiescence duration and the latency to first move also *decreased* monotonically (Figs. 6 and 7). There are significant differences from P3 to P6: movement duration was more than tripled, movement distance increased more than 4-fold, quiescence duration down by approximately 30% and movement latency shortened to one-sixth of the P3 value.

During development pups can grow more tolerant to colder temperature and become more likely to move at older ages. We observed behaviors at the same room temperature as that in the animal room, where the ambient temperature is the same as the temperature inside cages housing the pups and their mother. During all the tests, no pup was observed to curl up, indicating that the room temperature was not sensed as cold by the testing subjects, regardless of age. When mouse pups are tested as a group, they tend to huddle up with littermates at low temperatures to keep warm. Under such test conditions, there is no significant difference between the numbers or the sizes (measured as perimeter) of the huddling aggregates, or ultrasonic vocalization between P4 and P8 pups [57]. Similarly in rats, thermoregulation is consistently poor up to P7 and improves significantly only afterward [58]. These observations in mice and rats indicate that the development of thermoregulation during our observed period of P3-P6 is insignificant and cannot account for the development of the behaviors we observed. Indeed, in rats, at least, it has been reported that environmental temperature had a minimal influence on the degree of behavioral arousal seen in either familiar or unfamiliar environments [59]. Thus, mice progressed from virtually *not*-arousable at P3 to readily aroused at P6 due to the maturation of CNS arousal systems, rather than development of thermoregulation.

The development of neuronal capability to fire spike trains

One major finding of the present study is the evolution of NGC neurons' capability to fire repeatedly in spike trains during the neonatal time window. The capability of neurons to fire repetitively may involve several ion channels, including the rapid activating K^+ (A-current) channel, delayed rectifier, Ca^{++}-activated K^+ channels, certain Ca^{++} and Na^+ channel subtypes, leak K^+ currents, and others [60]. But, for NGC neurons, changes in A-current do not correlate with the progress of neuronal capability to fire spike trains or do arousal-related behaviors (Table 2). In tightly packed brain or brain slices, K^+ that leaked from cells is trapped in the narrow intercellular space and can cause depolarization and facilitate repetitive firing. In a parallel study using cultures of neurons dissociated from the hindbrain of mouse embryos, we found neurons developed the capability to fire spike train in a similar manner, though at different time course (results not shown). Here, K^+ would leak into open space and would not have any significant contribution to membrane potential. Thus, leak K^+ channels do not seem to be important for repetitive firing for hindbrain/NGC neurons. Ca^{++}-activated K^+ channels do not seem to be important, either because, throughout the present study, we have not seen obvious afterhyperpolarizations (for example, see Fig. 1, b and c) i.e. signs of the activation of these channels. Also, the development of NGC neurons' capability to fire single APs did not progress in an orderly time course or correlate with the development of arousal behaviors, indicating that the development of voltage-gated Na^+ channels alone, required for an AP, is not sufficient. In contrast to all these, the delayed rectifier developed in an orderly monotonic fashion, correlated with the development of repeated firing and arousal-related behaviors (Table 1 and 3). We believe the delayed rectifier K^+ channel and its corresponding gene, probably Kv2 [61], are the best targets for manipulating NGC neurons capability to fire spike train in evaluating whether the development of this neuronal characteristic is causally related to the development of arousal behaviors.

The mechanism of NGC neurons inducing arousal

Previous studies [62,63] have shown that medullary reticulospinal actions foster increased behavioral reactivity in the following way: That electrical stimulation of hindbrain reticular formation neurons potentiate motoneuronal responses to a given strength of segmental stimulus input. That is, descending signals from the medullary reticular formation effectively increase the slope of the stimulus-response curve. In addition, optogenetic or electrical excitation or disinhibition of NGC neurons modulate the cortical EEG of the deeply anesthetized animal from slow wave or burst suppression mode to activated high frequency activity [17]. All of these demonstrations were in the adult. It appears that during the neonatal developmental period studied in the present paper, the increasing excitability of NGC neurons allows them to play the roles demonstrated in the previous papers thus to permit the animals studied here to be active behaviorally as measured here.

Comments on methods

To study relationships between mouse brain neurons and behaviors, an ideal way is to record NGC neurons in conscious mice to observe both neuronal activity and animal behaviors simultaneously. This can be done with chronically implanted electrodes or the "head-fixed

method" [64,65]. The former method requires lengthy recovery time and hence, is impractical or impossible for P3-P6 pups. The latter method records from a neuron(s) by lowering a recording electrode blindly into the brain until some activity is detected. We have, in fact, used this method to study the activity of NGC neurons and behaviors, simultaneously, in adult mice [17]. This method, however, will sample only neurons capable of spontaneous firing of action potential. Since NGC neurons P3-P6 are silent and we are assessing their excitability as a function of age this method is obviously not suitable. We therefore used what we considered the next best way – using brain slices that contain NGC. In the predominant absence of reticular fibers at early life, NGC neurons can be easily visualized. This, together with the help of infrared differential interference contrast (IR-DIC) microscopy, and with anatomical landmarks, makes the patching on silent NGC neurons easy.

To ensure that NGC neurons are recorded, the use of genetically engineered mice with NGC neurons specifically labeled with a marker(s) would be ideal. To our best knowledge, there is only one such mouse line, which has some NGC neurons labeled with Chx10 [66]. However, since Chx10 marker labels only a subpopulation (40%) of NGC neurons, study of such neurons would lead to biased results. The marker is non-specific for NGC neurons; it also labels neurons elsewhere. More importantly, Chx10 labeled (V2a) brainstem neurons exert inhibitory influence on locomotion [67], a function opposite of that expected of neurons involved in arousal. Since we intended to study large NGC neurons that may regulate arousal, neurons with Chx10 marker are of little use. We have been working very hard in attempts to generate a mouse line with marked NGC neurons, but in spite of our attempts, such mice are not yet available.

Inference that NGC neuronal maturation fosters the development of behavioral arousal

In addition to the correlations discussed above, between the expression of Na^+ channels in combination with the development of delayed rectifier K^+ channels in NGC neurons and the development of arousal-related behaviors during P3-P6, the *causal* relationship between NGC neurons and arousal has already been indicated by several pieces of evidence in the literature. The importance NGC in CNS arousal has been reviewed [9] [17]. Regarding the main hallmark of behavioral arousal, the initiation of motor activity, microtransections of descending reticulospinal tracts resulting in degeneration of NGC neurons caused motor disturbances indicating that NGC neurons are involved in movement initiation [68]. This indication is further supported by other reports [16,19,66]. Conversely, in the anesthetized rat, stimulation of NGC caused the appearance of high frequency, low amplitude, 'waking' electroencephalograms [20]. In behaving rats, stimulation of NGC can increase and generate various behaviors including behavioral arousal [69]. These findings are recently further reinforced and extended to mice by the facts that both electrical and chemical stimulation could evoke arousal-related behaviors [17]. Putting together the close correlations of NGC electrophysiology and arousal reported in Results, and the literature extant, it becomes clear that NGC neuronal development is critically important for the development of behavioral arousal in the neonate.

Acknowledgments

This work has been supported by a grant HD 05751 from NIH (DWP, LMK), a grant RO1 NS094655-01 (DPC), a grant from the New York Neuroscience Foundation (IT), grants from National Natural Science Foundation of China (code:81301108) and Shanghai Natural Science Foundation, china (code:13ZR1406500) (XL) and grants from National Natural Science Foundation of China (Code: 31271188)and Shanghai Municipal Science and Technology Commission, China (Code:13DJ1400300) (XW). Illuminating discussions with Prof. David Gadsby are much appreciated.

Abbreviations

ACSF	artificial cerebrospinal fluid
AP	action potential
EEG	electroencephalogram
EPSC	excitatory postsynaptic current
GABA	γ-aminobutyric acid
Glut	glutamate
HA	histamine
MKT	Mann-Kendall test for Trend
NGC	nucleus gigantocellularis
NMDA	N-methyl-D-aspartate
NPk	negative peak
PhE	phenylephrine
PPk	positive peak
SSt	steady state
Vh	holding potential
Vm	membrane potential

References

1. Patisaul HB, Polston EK. Influence of endocrine active compounds on the developing rodent brain. Brain Res Rev. 2008; 57:352–362. [PubMed: 17822772]
2. Foecking EM, McDevitt MA, Acosta-Martinez M, Horton TH, Levine JE. Neuroendocrine consequences of androgen excess in female rodents. Horm Behav. 2008; 53:673–692. [PubMed: 18374922]
3. Scattoni ML, Crawley J, Ricceri L. Ultrasonic vocalizations: A tool for behavioural phenotyping of mouse models of neurodevelopmental disorders. Neurosci Biobehav Rev. 2009; 33:508–515. [PubMed: 18771687]
4. Pfaff D, Ribeiro A, Matthews J, Kow LM. Concepts and mechanisms of generalized central nervous system arousal. Ann N Y Acad Sci. 2008; 1129:11–25. [PubMed: 18591465]

5. Aston-Jones G. Brain structures and receptors involved in alertness. Sleep Med. 2005; 6:S3–S7. [PubMed: 16140243]
6. de Lecea L, Carter ME, Adamantidis A. Shining light on wakefulness and arousal. Biol Psychiatry. 2012; 71:1046–1052. [PubMed: 22440618]
7. Harris GC, Aston-Jones G. Arousal and reward: A dichotomy in orexin function. Trends Neurosci. 2006; 29:571–577. [PubMed: 16904760]
8. Jones BE. Arousal systems. Front Biosci. 2003; 1:s438–s451.
9. Pfaff DW, Martin EM, Faber D. Origins of arousal: Roles for medullary reticular neurons. Trends Neurosci. 2012; 35:468–476. [PubMed: 22626543]
10. Jones BE, Yang TZ. The efferent projections from the reticular formation and the locus coeruleus studied by anterograde and retrograde axonal transport in the rat. J Comp Neurol. 1985; 242:56–92. [PubMed: 2416786]
11. Abzug C, Maeda M, Peterson BW, Wilson VJ. Cervical branching of lumbar vestibulospinal axons. J Physiol. 1974; 243:499–522. [PubMed: 4449072]
12. Martin EM, Devidze N, Shelley DN, Westberg L, Fontaine C, Pfaff DW. Molecular and neuroanatomical characterization of single neurons in the mouse medullary gigantocellular reticular nucleus. J Comp Neurol. 2011; 519:2574–2593. [PubMed: 21456014]
13. Peterson BW. Current approaches and future directions to understanding control of head movement. Prog Brain Res. 2004; 143:369–381. [PubMed: 14653180]
14. Valverde F. Reticular formation of the albino rat's brain stem cytoarchitecture and corticofugal connections. J Comp Neurol. 1962; 119:25–53. [PubMed: 13924447]
15. Martin EM, Pavlides C, Pfaff D. Multimodal sensory responses of nucleus reticularis gigantocellularis and the responses' relation to cortical and motor activation. J Neurophysiol. 2010; 103:2326–2338. [PubMed: 20181730]
16. Vertes RP. Selective firing of rat pontine gigantocellular neurons during movement and rem sleep. Brain Res. 1977; 128:146–152. [PubMed: 194653]
17. Calderon DP, Proekt A, Hudson A, DWP. Gigantocellular neurons awaken the brain from pharmacologically-induced coma. Nat neurosci. 2016 Under Revision.
18. Crone SA, Zhong G, Harris-Warrick R, Sharma K. In mice lacking v2a interneurons, gait depends on speed of locomotion. J Neurosci. 2009; 29:7098–7109. [PubMed: 19474336]
19. Vertes RP. Brain stem gigantocellular neurons: Patterns of activity during behavior and sleep in the freely moving rat. J Neurophysiol. 1979; 42:214–228. [PubMed: 219157]
20. Wu HB, Stavarache M, Pfaff DW, Kow LM. Arousal of cerebral cortex electroencephalogram consequent to high-frequency stimulation of ventral medullary reticular formation. Proc Natl Acad Sci U S A. 2007; 104:18292–18296. [PubMed: 17984058]
21. Litvin Y, Cataldo G, Pfaff DW, Kow LM. Estradiol regulates responsiveness of the dorsal premammillary nucleus of the hypothalamus and affects fear- and anxiety-like behaviors in female rats. Eur J Neurosci. 2014; 40:2344–2351. [PubMed: 24862453]
22. Zhou J, Kow LM, Vannucci SJ, Pfaff D, Martin EM. Arousal-related reticular neurons during reduced oxygen tension: Resilience and recovery of electrical activity. Dev Neurosci. 2009; 31:255–258. [PubMed: 19546562]
23. Hardy SP, deFelipe C, Valverde MA. Inhibition of voltage-gated cationic channels in rat embryonic hypothalamic neurones and c1300 neuroblastoma cells by triphenylethylene antioestrogens. FEBS Lett. 1998; 434:236–240. [PubMed: 9742930]
24. Milescu LS, Bean BP, Smith JC. Isolation of somatic Na^+ currents by selective inactivation of axonal channels with a voltage prepulse. J Neurosci. 2010; 30:7740–7748. [PubMed: 20519549]
25. Kow LM, Pfaff DW. Responses of ventromedial hypothalamic neurons in vitro to norepinephrine: Dependence on dose and receptor type. Brain Res. 1987; 413:220–228. [PubMed: 3038269]
26. Kow LM, Pfaff DW. Responses of hypothalamic paraventricular neurons in vitro to norepinephrine and other feeding-relevant agents. Physiol Behav. 1989; 46:265–271. [PubMed: 2574890]
27. Ben-Ari Y. Excitatory actions of gaba during development: The nature of the nurture. Nat Rev Neurosci. 2002; 3:728–739. [PubMed: 12209121]

28. Leinekugel X, Tseeb V, Ben-Ari Y, Bregestovski P. Synaptic gabaa activation induces Ca^{2+} rise in pyramidal cells and interneurons from rat neonatal hippocampal slices. The Journal of Physiology. 1995; 487:319–329. [PubMed: 8558466]
29. Nunez LJ, Bambrick LL, Krueger BK, McCarthy MM. Prolongation and enhancement of gamma-aminobutyric acid(a) receptor mediated excitation by chronic treatment with estradiol in developing rat hippocampal neurons. Eur J Neurosci. 2005; 21:3251–3261. [PubMed: 16026463]
30. Dupré C, Lovett-Barron M, Pfaff DW, Kow L-M. Histaminergic responses by hypothalamic neurons that regulate lordosis and their modulation by estradiol. Proc Natl Acad Sci U S A. 2010; 107:12311–12316. [PubMed: 20562342]
31. Serafin M, Khateb A, Muhlethaler M. Electrophysiology and lucifer yellow injection of nucleus gigantocellularis neurones in an isolated and perfused guinea pig brain in vitro. Neurosci Lett. 1990; 120:5–8. [PubMed: 2293091]
32. Serafin M, Vidal PP, Mohlethaler M. Electrophysiological study of nucleus gigantocellularis neurons in guinea-pig brainstem slices. Neuroscience. 1996; 73:797–805. [PubMed: 8809799]
33. Arancillo M, White JJ, Lin T, Stay TL, Sillitoe RV. In vivo analysis of purkinje cell firing properties during postnatal mouse development. J Neurophysiol. 2015; 113:578–591. [PubMed: 25355961]
34. Fry M. Developmental expression of Na^+ currents in mouse purkinje neurons. Eur J Neurosci. 2006; 24:2557–2566. [PubMed: 17100843]
35. McKay BE, Turner RW. Physiological and morphological development of the rat cerebellar purkinje cell. J Physiol. 2005; 567:829–850. [PubMed: 16002452]
36. McCormick DA, Prince DA. Post-natal development of electrophysiological properties of rat cerebral cortical pyramidal neurones. J Physiol. 1987; 393:743–762. [PubMed: 2895811]
37. Pre D, Nestor MW, Sproul AA, Jacob S, Koppensteiner P, Chinchalongporn V, Zimmer M, Yamamoto A, Noggle SA, Arancio O. A time course analysis of the electrophysiological properties of neurons differentiated from human induced pluripotent stem cells (ipscs). PLoS One. 2014; 9:e103418–e103431. [PubMed: 25072157]
38. Strubing C, Ahnert-Hilger G, Shan J, Wiedenmann B, Hescheler J, Wobus AM. Differentiation of pluripotent embryonic stem cells into the neuronal lineage in vitro gives rise to mature inhibitory and excitatory neurons. Mech Dev. 1995; 53:275–287. [PubMed: 8562428]
39. Song M, Mohamad O, Chen D, Yu SP. Coordinated development of voltage-gated Na^+ and K^+ currents regulates functional maturation of forebrain neurons derived from human induced pluripotent stem cells. Stem Cells Dev. 2013; 22:1551–1563. [PubMed: 23259973]
40. Takazawa T, Croft GF, Amoroso MW, Studer L, Wichterle H, Macdermott AB. Maturation of spinal motor neurons derived from human embryonic stem cells. PLoS One. 2012; 7:3.
41. Kawaguchi A, Asano H, Matsushima K, Wada T, Yoshida S, Ichida S. Enhancement of sodium current in ng108-15 cells during neural differentiation is mainly due to an increase in nav1.7 expression. Neurochem Res. 2007; 32:1469–1475. [PubMed: 17404832]
42. Kow LM, Devidze N, Pataky S, Shibuya I, Pfaff DW. Acute estradiol application increases inward and decreases outward whole-cell currents of neurons in rat hypothalamic ventromedial nucleus. Brain Res. 2006; 20:1–11.
43. Biella G, Di Febo F, Goffredo D, Moiana A, Taglietti V, Conti L, Cattaneo E, Toselli M. Differentiating embryonic stem-derived neural stem cells show a maturation-dependent pattern of voltage-gated sodium current expression and graded action potentials. Neuroscience. 2007; 149:38–52. [PubMed: 17870247]
44. Hanani M, Francke M, Hartig W, Grosche J, Reichenbach A, Pannicke T. Patch-clamp study of neurons and glial cells in isolated myenteric ganglia. Am J Physiol Gastrointest Liver Physiol. 2000; 278:G644–G651. [PubMed: 10762619]
45. Crill WE. Persistent sodium current in mammalian central neurons. Annu Rev Physiol. 1996; 58:349–362. [PubMed: 8815799]
46. Taddese A, Bean BP. Subthreshold sodium current from rapidly inactivating sodium channels drives spontaneous firing of tuberomammillary neurons. Neuron. 2002; 33:587–600. [PubMed: 11856532]

47. Afshari FS, Ptak K, Khaliq ZM, Grieco TM, Slater NT, McCrimmon DR, Raman IM. Resurgent na currents in four classes of neurons of the cerebellum. J Neurophysiol. 2004; 92:2831–2843. [PubMed: 15212420]
48. Raman IM, Bean BP. Inactivation and recovery of sodium currents in cerebellar purkinje neurons: Evidence for two mechanisms. Biophys J. 2001; 80:729–737. [PubMed: 11159440]
49. Kim J, Wei DS, Hoffman DA. Kv4 potassium channel subunits control action potential repolarization and frequency-dependent broadening in rat hippocampal ca1 pyramidal neurones. J Physiol. 2005; 569:41–57. [PubMed: 16141270]
50. Mitterdorfer J, Bean BP. Potassium currents during the action potential of hippocampal ca3 neurons. J Neurosci. 2002; 22:10106–10115. [PubMed: 12451111]
51. Kuo JJ, Schonewille M, Siddique T, Schults AN, Fu R, Bar PR, Anelli R, Heckman CJ, Kroese AB. Hyperexcitability of cultured spinal motoneurons from presymptomatic als mice. J Neurophysiol. 2004; 91:571–575. [PubMed: 14523070]
52. Meehan CF, Sukiasyan N, Zhang M, Nielsen JB, Hultborn H. Intrinsic properties of mouse lumbar motoneurons revealed by intracellular recording in vivo. J Neurophysiol. 2010; 103:2599–2610. [PubMed: 20164401]
53. Miles GB, Yohn DC, Wichterle H, Jessell TM, Rafuse VF, Brownstone RM. Functional properties of motoneurons derived from mouse embryonic stem cells. J Neurosci. 2004; 24:7848–7858. [PubMed: 15356197]
54. Kawamura Y, Nakayama H, Hashimoto K, Sakimura K, Kitamura K, Kano M. Spike timing-dependent selective strengthening of single climbing fibre inputs to purkinje cells during cerebellar development. Nat Commun. 2013; 4:2732–2744. [PubMed: 24225482]
55. Sokoloff G, Blumberg MS, Boline EA, Johnson ED, Streeper NM. Thermoregulatory behavior in infant norway rats (rattus norvegicus) and syrian golden hamsters (mesocricetus auratus): Arousal, orientation, and locomotion. J Comp Psychol. 2002; 116:228–239. [PubMed: 12234072]
56. Spigelman I, Zhang L, Carlen PL. Patch-clamp study of postnatal development of ca1 neurons in rat hippocampal slices: Membrane excitability and K^+ currents. J Neurophysiol. 1992; 68:55–69. [PubMed: 1517828]
57. Harshaw C, Alberts JR. Group and individual regulation of physiology and behavior: A behavioral, thermographic, and acoustic study of mouse development. Physiol Behav. 2012; 106:670–682. [PubMed: 22580514]
58. Kleitman N, Satinoff E. Thermoregulatory behavior in rat pups from birth to weaning. Physiol Behav. 1982; 29:537–541. [PubMed: 7178260]
59. Campbell RA, Raskin LA. Ontogeny of behavioral arousal: The role of environmental stimuli. J Comp Physiol Psychol. 1978; 92:176–184. [PubMed: 627636]
60. Bean BP. The action potential in mammalian central neurons. Nat Rev Neurosci. 2007; 8:451–465. [PubMed: 17514198]
61. Blaine JT, Ribera AB. Kv2 channels form delayed-rectifier potassium channels in situ. J Neurosci. 2001; 21:1473–1480. [PubMed: 11222637]
62. Brink EE, Pfaff DW. Supraspinal and segmental input to lumbar epaxial motoneurons in the rat. Brain Res. 1981; 226:43–60. [PubMed: 7296299]
63. Cohen MS, Schwartz-Giblin S, Pfaff DW. Brainstem reticular stimulation facilitates back muscle motoneuronal responses to pudendal nerve input. Brain Res. 1987; 405:155–158. [PubMed: 3567589]
64. Blumberg MS, Sokoloff G, Tiriac A, Del Rio-Bermudez C. A valuable and promising method for recording brain activity in behaving newborn rodents. Dev Psychobiol. 2015; 57:506–517. [PubMed: 25864710]
65. Karlsson KA, Blumberg MS. Active medullary control of atonia in week-old rats. Neuroscience. 2005; 130:275–283. [PubMed: 15561443]
66. Bretzner F, Brownstone RM. Lhx3-chx10 reticulospinal neurons in locomotor circuits. J Neurosci. 2013; 33:14681–14692. [PubMed: 24027269]
67. Bouvier J, Caggiano V, Leiras R, Caldeira V, Bellardita C, Balueva K, Fuchs A, Kiehn O. Descending command neurons in the brainstem that halt locomotion. Cell. 2015; 163:1191–1203. [PubMed: 26590422]

68. Zemlan FP, Kow L-M, Morrell JI, Pfaff DW. Descending tracts of the lateral columns of the rat spinal cord: A study using the horseradish peroxidase and silver impregnation techniques. J Anat. 1979; 128:489–512. [PubMed: 89111]

69. Roberts VJ. Ngc-evoked nociceptive behaviors: I. Effect of nucleus gigantocellularis stimulation. Physiol Behav. 1992; 51:65–71. [PubMed: 1311111]

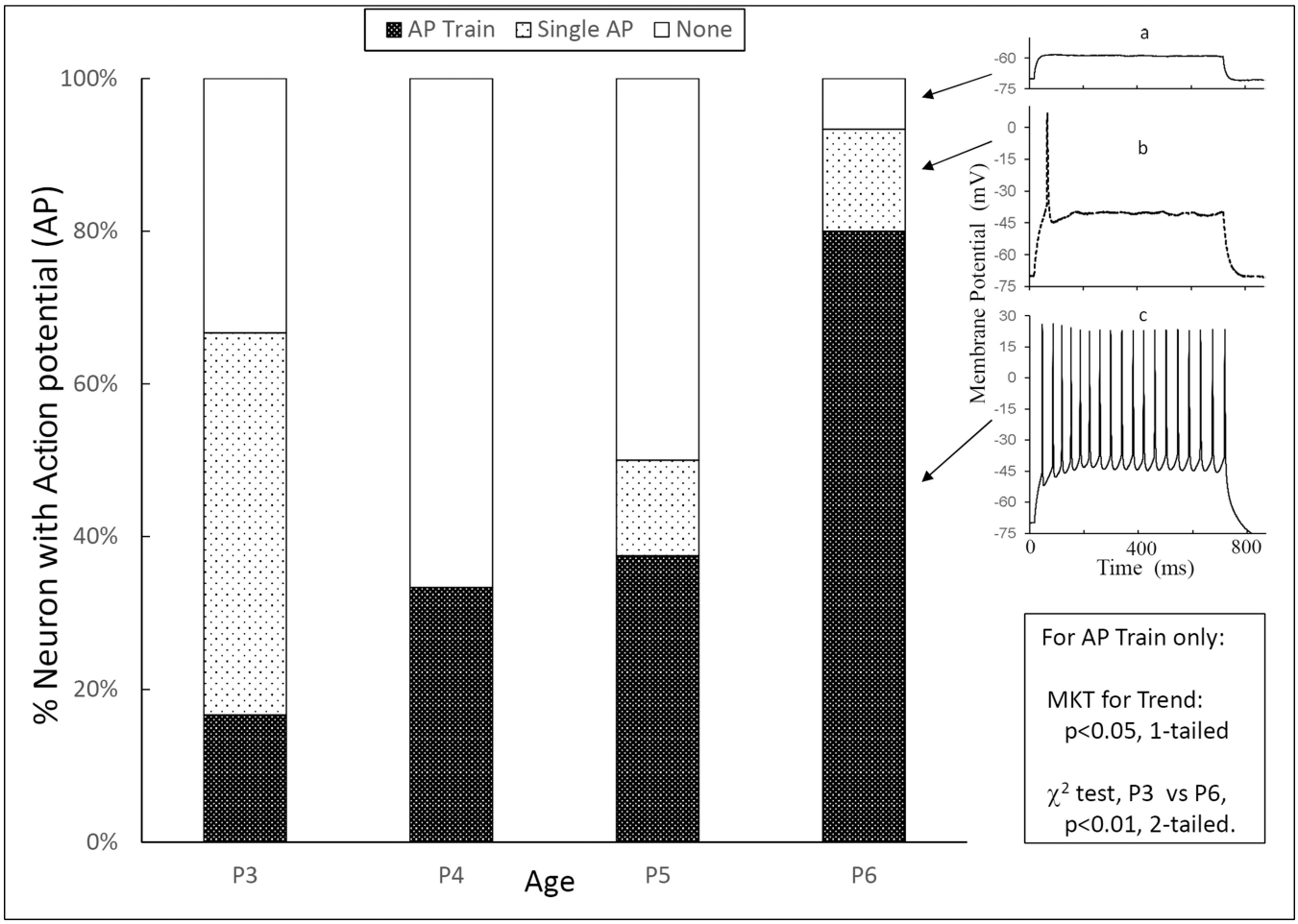

Fig. 1. Capability of neurons to fire AP train increased over P3 to P6 of age

Percentage of recorded neurons capable of firing AP train increased monotonically and significant statistically (Mann-Kendall, or MKT, test for Trend, enclosed insert) from P3 through P6. Neither the fraction of neurons capable of firing no or single AP, nor that of firing both single and AP train combined was changing monotonically (Table 2). Typical examples of neurons firing no AP (insert a), single AP (insert b), or AP train (insert c) are illustrated in the inserts. The examples in the insert also illustrate general differences between single AP and AP train in amplitude (peak below 10 mV for single vs above 20 mV for train) and the threshold (above −45 mV for single vs below −40 mV for the first AP in the train).

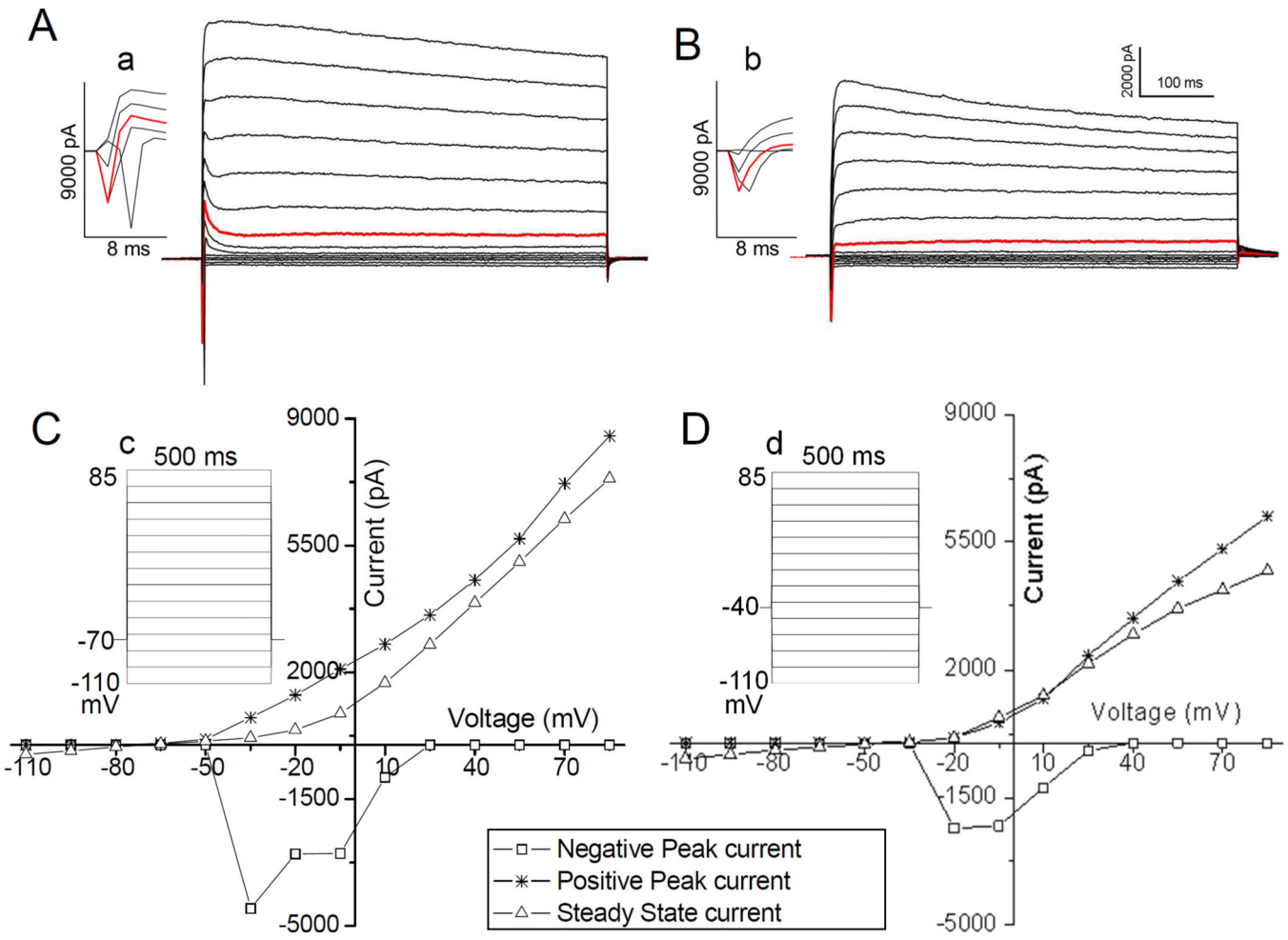

Fig. 2. Example of currents generated by I-V step from holding potential (Vh) at −70 mV and −40 mV

Current traces (A and B) and the corresponding I-V plots (C and D) from both protocols (**inserts Cc and Dd**) are obtained from a single, typical neuron. Traces in A and the corresponding I-V plot (C) were generated with the protocol (see insert Cc) starting from Vh = −70 mV, while those of B and D were from the protocol (insert d) with Vh= −40 mV. In A, the middle traces, from the second trace below through the third trace above the high-lighted one, the current response is initiated by a rapid upswing (i.e., rapid activating current). These upswing are expanded and illustrated in the **insert Aa** and reflected as the gaps between PPk and SSt curves in I-V plot C. In contrast, these upswings can no longer be seen in B or the **insert Bb**, and are reflected as the vanishing of the PPk-SSt gaps from −35 mV through 25mV in I-V plot D. All these indicating that rapid activating currents were inactivated at Vh of −40 mV. Note that after the rapid activating currents disappeared in A or inactivated in B, traces, especially upper ones, are still initiated with a gentle “peak”. These peak currents are slower than the rapid activating currents and are referred to as “fast activating currents”. They are reflected as the PPk-SSt gaps at 40 mV through 85 mV in I-V plots C and D. Traces in A and B are plotted in same scales, which are shown in the upper right corner of B.

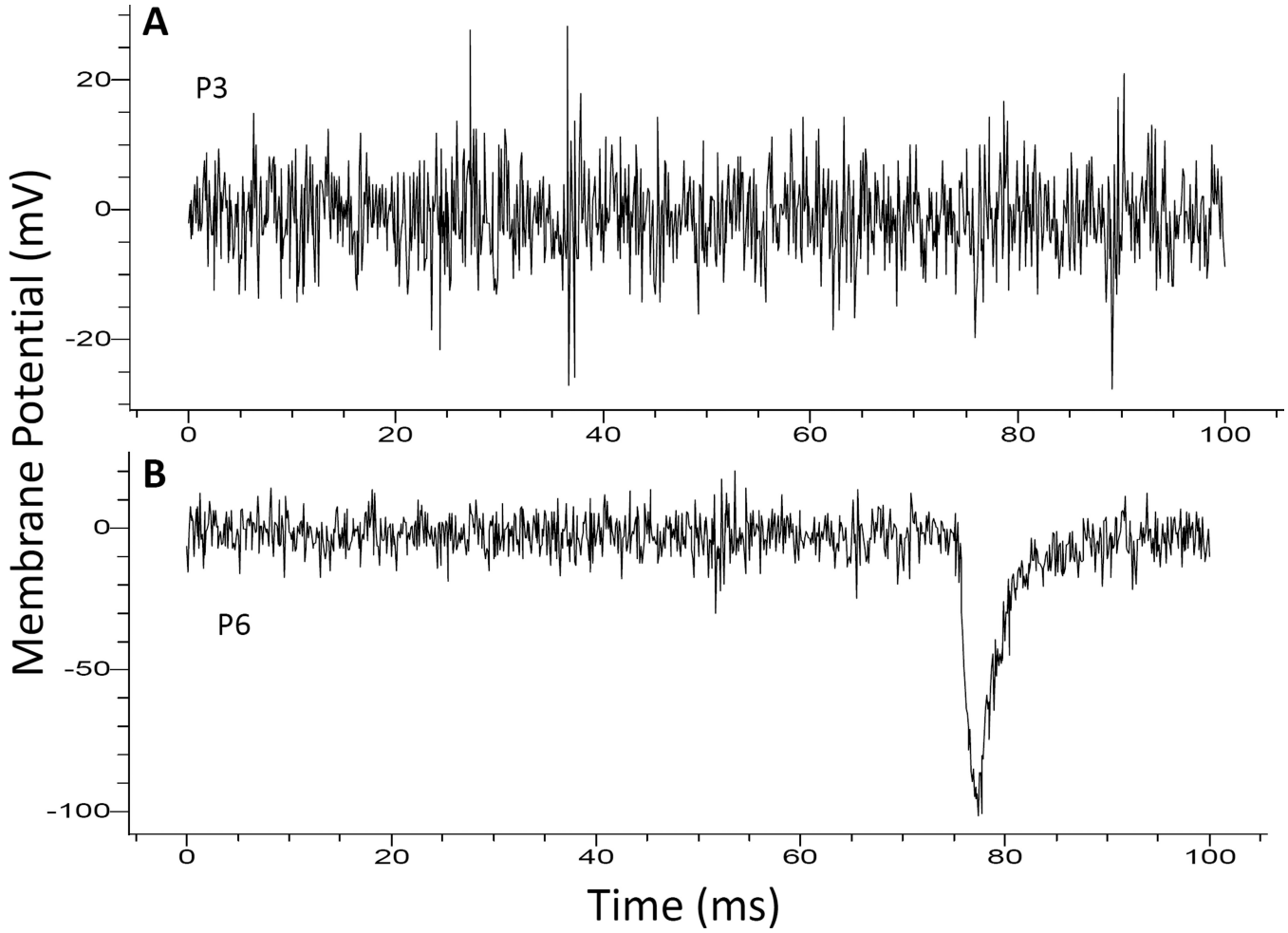

Fig. 3. Recording of EPSC from NGC neurons

Some neurons like the one shown in A did not show EPSC. Others showed EPSC of various amplitude and frequency. One example with a large EPSC is illustrated in B.

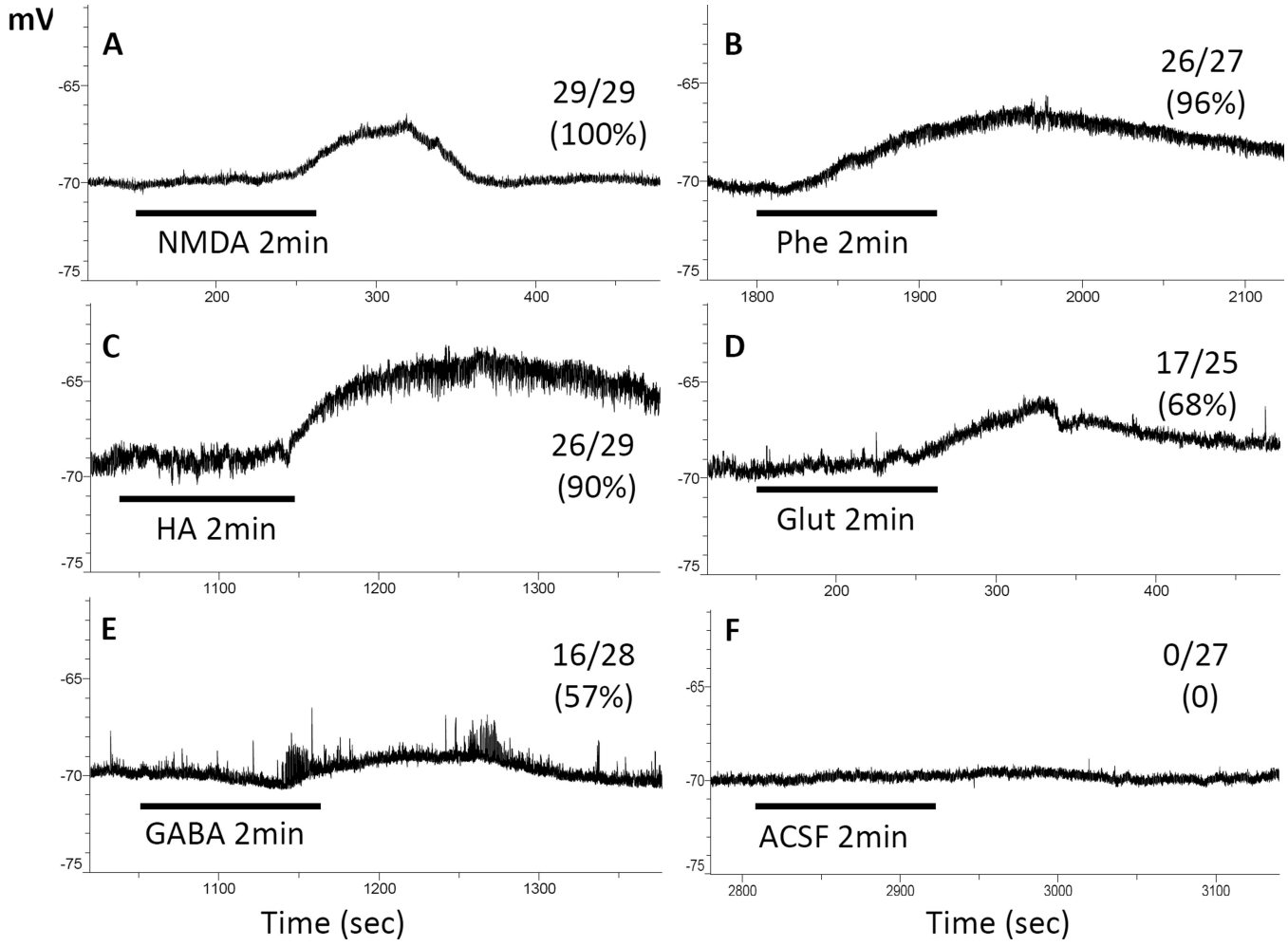

Fig. 4. Responses of NGC neurons to a battery of transmitter agents

Traces are membrane potential recorded from NGC neurons, which frequently responded with depolarization to the agents. The bar beneath the trace indicates the time and the duration (always 2 min) when the agent indicated below the bar was bath applied. The numbers above or below the end of each trace are the fraction and percentage of the neurons responded. In A through E, neurons were tested with one of the agents. In F, the neuron was treated with the vehicle, ACSF, to serve as control

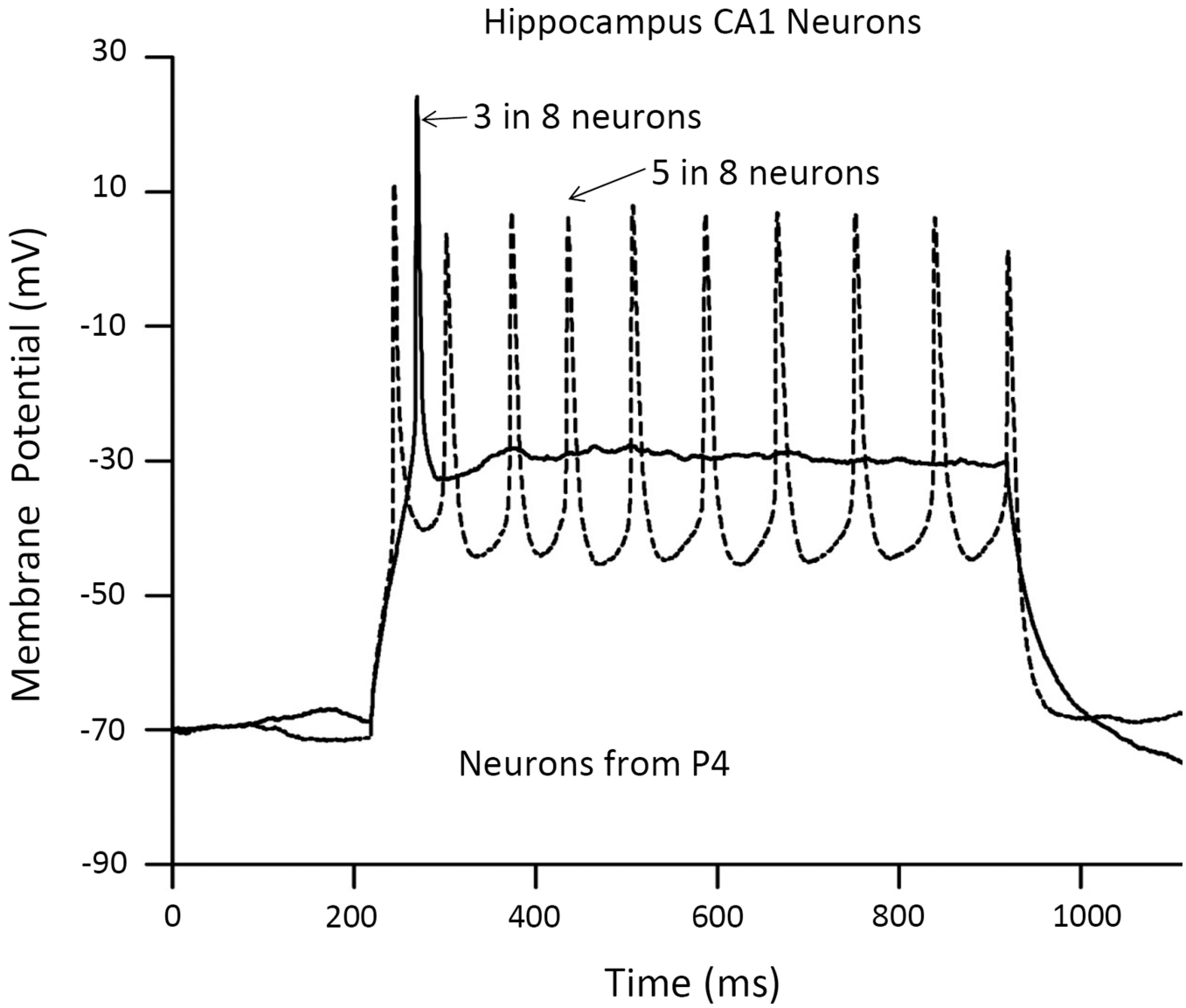

Fig. 5. Induction of AP by current injection (70 pA) of CA1 neurons from hippocampus of P4 mice

All 8 hippocampal neurons recoded were capable of firing AP in response to an injection of the same amount of current, 70 pA, as those NGC neurons shown in Fig. 1. This responsiveness is similar and surpasses that of P6 NGC neurons in that 100% of hippocampal neurons were capable of firing AP, indicating that hippocampal neurons are more advanced in development.

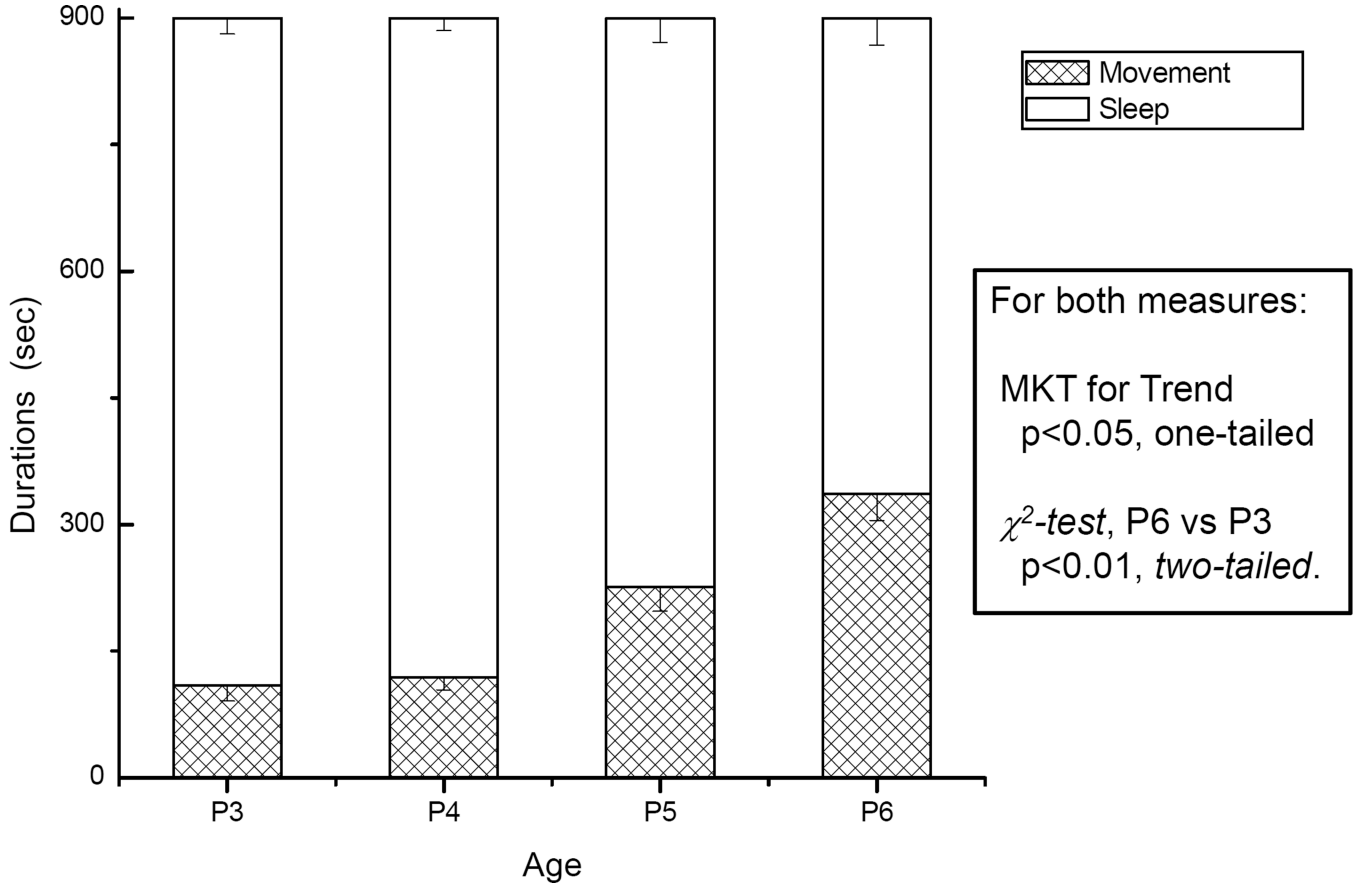

Fig. 6. Mice quiescence time decreases and movement time gets increases over P3 – P6

Durations of quiescence and total movement were observed for a total of 900 second. Results are presented as average and with SEM as error bar. N = 14 for all age groups.

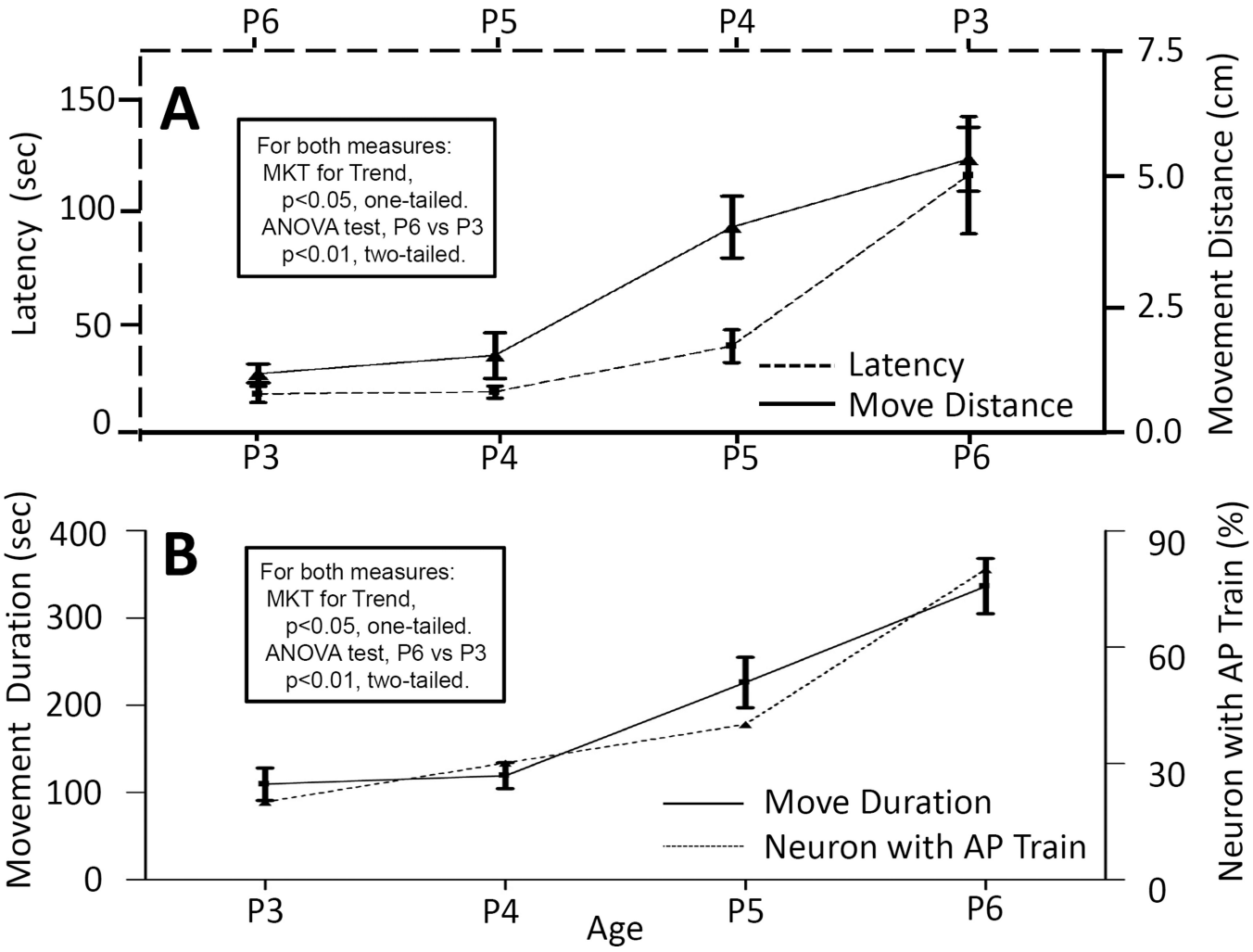

Fig. 7. Correlations between behavior measures and the capability of NGC neurons to fire AP train

For clarity, three behavior measures are divided into panels A and B. In A, the age scale for latency to movement (dashed line) is reversed. Changes for all measures over the age range are monotonical and significant (MKT, of Mann-Kendall test for Trend, all $p<0.05$, one-tailed). For each measure, the value on P3 is significantly different from that on P6 (ANOVA, all $p<0.01$, two-tailed). As presented in Table 3, the monotonical change of neurons with AP train is significantly (Spearman rank correlation coefficient test, all $p<0.05$, one-tailed) correlated with that for all behavior measures. Error bars represent SEM. For all behavior measures, n = 14; for neurons with AP train, n = 12 to 18.

Table 1

Bioelectrical characteristics of NGC neurons that changed in Trends over P3-P6 of age. Results are presented as M±SEM (n) in this and other tables.

		P3	P4	P5	P6	Trend[a]	P3 vs P6[b]
Action potential	Neurons with AP train (%)	17 (2/12)	33 (6/18)	38 (6/16)	80 (12/15)	p< 0.05	p<0.01[c]
	Amplitude (mV)	47.7 ± 2.0 (8)	49.0 ± 3.0 (6)	52.0 ± 2.9 (8)	56.0 ± 2.5 (14)	p< 0.05	p<0.05
	Threshold (mV)	−30.8 ± 1.8 (8)	−34.2 ± 1.0 (6)	−37.2 ± 2.1 (8)	−38.2 ± 2.4 (13)	p< 0.05	p<0.01
Currents by single voltage step	Inward (pA)	−1366 ± 144 (12)	−2099 ± 292 (18)	−2207 ± 291 (16)	−2689 ± 270 (15)	p< 0.05	p<0.001
	Outward (pA)	1427 ± 353 (12)	3220 ± 598 (18)	4132 ± 730 (16)	5312 ± 852 (15)	p< 0.05	p<0.001
Currents by multiple voltage steps	Neg Pk (pA) Vh −70 mV[e]	−1110 ± 243 (12)	−2075 ± 27 (18)	−2389 ± 351 (16)	−3161 ± 443 (15)	p< 0.05	p<0.001
	Neg Pk (pA) Vh −40 mV	−1273 ± 88 (12)	−1667 ± 250 (18)	−1790 ± 209 (16)	−2461 ± 344 (15)	p< 0.05	p<0.01
	Steady State Current (pA)	3160 ± 299 (12)	4447 ± 389 (18)	4473 ± 515 (16)	4829 ± 438 (15)	p< 0.05	p<0.01
EPSCs	Amplitude (pA)	57.9 ± 11.1 (6)	49.3 ± 3.1 (39)	49.2 ± 4.3 (18)	40.8 ± 1.8 (28)	p<0.05	p<0.01
	Area (arbitrary unit)	97.6 ± 28.6 (6)	91.4 ± 10.0 (39)	67.7 ± 6.2 (18)	55.6 ± 3.5 (28)	p<0.05	p<0.01

[a] Mann-Kendall test for Trend, one-tailed.

[b] ANOVA, two-tailed.

[c] χ^2 test, 2-tailed.

Dev Neurosci. Author manuscript; available in PMC 2017 October 28.

Table 2

Bioelectrical characteristics of NGC neurons that did not change in Trends over P3-P6 of age. Results are presented as M±SEM (n) in this and other tables.

		P3	P4	P5	P6	Trend[a]	P3 vs P6
Action Potential	Neurons with single AP (%)	50 (6/12)	0 (0/18)	13 (2/15)	14 (2/14)	ns	p<0.05[c]
Currents by multiple voltage steps	Positive Peak (pA)	3501 ± 245 (12)	4653 ± 478 (18)	4594 ± 577 (16)	5327 ± 543 (15)	ns	p<0.01[b]
	Rapid activating Current (pA)	913 ± 126 (12)	811 ±149 (17)	684 ± 97 (14)	940 ± 122 (15)	ns	ns[b]
	Fast activating Current (pA)	341 ± 180 (12)	206 ±167 (18)	121 ± 219 (16)	498 ± 161 (15)	ns	ns[b]
	Negative Peak Position (pA)	−18.7 ± 2.9 (12)	−29.2 ± 2.5 (18)	−37.0 ± 2.0 (15)	−29.6 ± 4.0 (14)	ns	p<0.05[b] 1-tailed
EPSCs	Neurons with EPSCs, % (n/n)	42% (5/12)	39% (7/18)	38% (6/16)	43% (6/14)	ns	ns[c]
	EPSCs frequency (Hz)	2.4 ± 0.4 (5)	10.9 ± 4.7 (7)	6.0 ± 2.0 (6)	9.3 ± 3.4 (6)	ns	ns[b]
Neurons responded to: % (n/n)	HA	100% (7/7)	89% (8/9)	83% (5/6)	86% (6/7)	ns	ns[c]
	Glut	67% (4/6)	71% (5/7)	67% (4/6)	67% (4/6)	ns	ns[c]
	PhE	100% (6/6)	100% (8/8)	100% (6/6)	86% (6/7)	ns	ns[c]
	GABA	29% (2/7)	75% (6/8)	67% (4/6)	57% (4/7)	ns	ns[c]
	NMDA	100% (8/8)	100% (8/8)	100% (6/6)	100% (7/7)	ns	ns[c]

[a] Mann-Kendall test for Trend, one-tailed.

[b] ANOVA, two-tailed.

[c] χ^2 test, 2-tailed.

Table 3

Measurements of arousal-indicative behaviors and the correlated bioelectrical characteristics of NGC neurons that changed in Trends over P3-P6 of age.

	Items observed		P3	P4	P5	P6	Trend[a]	P3 vs P6[b]
Arousal-related behaviors (all n=14)	Movement duration (sec)		109.6 ± 18.6	119.2 ±14.9	226.0 ± 28.7	336.6 ± 31.8	p< 0.05	p<0.001
	Movement distance (cm)		1.27 ± 0.18	1.62 ± 0.44	4.11 ± 0.60	5.42 ± 0.62	p< 0.05	p<0.001
	Latency to movement (sec)		119.3 ± 26.4	42.1 ± 7.4	21.4 ± 2.7	20.3 ± 3.7	p< 0.05	p<0.005
	Quiescence duration (sec)		7 9 0 .4 ± 18.6	780.8 ± 14.9	674.0 28.7	563.4 ± 31.8	p< 0.05	p<0.001
Bioelectrical characteristics of NGC neurons	Action potential	Neurons with AP train (%)	17 (2/12)	33 (6/18)	38 (6/16)	80 (12/15)	p< 0.05	p<0.01[c]
		Amplitude (mV)	47.7 ± 2.0 (8)	49.0 ± 3.0 (6)	52.0 ± 2.9 (8)	56.0 ± 2.5 (14)	p< 0.05	p<0.05
		Threshold (mV)	−30.8 ± 1.8 (8)	−34.2 ± 1.0 (6)	−37.2 ± 2.1 (8)	−38.2 ± 2.4 (13)	p< 0.05	p<0.01
	Currents by single voltage step	Inward (pA)	−1366 ± 144 (12)	−2099 ± 292 (18)	−2207 ± 291 (16)	−2689 ± 270 (15)	p< 0.05	p<0.001
		Outward (pA)	1427 ± 353 (12)	3220 ± 598 (18)	4132 ± 730 (16)	5312 ± 852 (15)	p< 0.05	p<0.001
	Currents by multiple voltage steps	Neg Pk (pA) Vh −70 mV[e]	−1110 ± 243 (12)	−2075 ± 27 (18)	−2389 ± 351 (16)	−3161 ± 443 (15)	p< 0.05	p<0.001
		Neg Pk (pA) Vh −40 mV	−1273 ± 88 (12)	−1667 ± 250 (18)	−1790 ± 209 (16)	−2461 ± 344 (15)	p< 0.05	p<0.01
		Steady State Current (pA)	3160 ± 299 (12)	4447 ± 389 (18)	4473 ± 515 (16)	4829 ± 438 (15)	p< 0.05	p<0.01
R_{Sr}[d], Any item vs any others			all p<0.05.					

[a] Mann-Kendall test for Trend, one-tailed.

[b] ANOVA, two-tailed.

[c] χ^2 test, 2-tailed.

[d] Spearman rank correlation coefficient, one-tailed. Each and any of the behavior measures is significantly correlated with each and any of the neuronal characteristics.